Published in final edited form as:
Dev Biol. 2014 February 15; 386(2): 448–460. doi:10.1016/j.ydbio.2013.12.038.

An Essential Role for Heat Shock Transcription Factor Binding Protein 1 (HSBP1) During Early Embryonic Development

Binnur Eroglu[1,2], **Jin-Na Min**[2,3], **Yan Zhang**[2,4], **Edyta Szurek**[5], **Demetrius Moskophidis**[2], **Ali Eroglu**[5,6], and **Nahid F. Mivechi**[1,2,6]

[1]Charlie Norwood VA Medical Center, One Freedom Way, Augusta, GA 30904

[2]Chaperone Biology, Georgia Regents University (GRU) Cancer Center, Medical College of Georgia (MCG), 1120 15th St., Augusta, GA 30912

[5]Institute of Molecular Medicine and Genetics, GRU, MCG

Abstract

Heat shock factor binding protein 1 (HSBP1) is a 76 amino acid polypeptide that contains two arrays of hydrophobic heptad repeats and was originally identified through its interaction with the oligomerization domain of heat shock factor 1 (Hsf1), suppressing Hsf1's transcriptional activity following stress. To examine the function of HSBP1 *in vivo*, we generated mice with targeted disruption of the *hsbp1* gene and examined zebrafish embryos treated with HSBP1-specific morpholino oligonucleotides. Our results show that *hsbp1* is critical for preimplantation embryonic development. Embryonic stem (ES) cells deficient in *hsbp1* survive and proliferate normally into the neural lineage *in vitro*; however, lack of *hsbp1* in embryoid bodies (EBs) leads to disorganization of the germ layers and a reduction in the endoderm-specific markers (such as α-fetoprotein). We further show that *hsbp1*-deficient mouse EBs and knockdown of HSBP1 in zebrafish leads to an increase in the expression of the neural crest inducers *Snail2*, *Tfap2*α and *Foxd3*, suggesting a potential role for HSBP1 in the Wnt pathway. The *hsbp1*-deficient ES cells, EBs and zebrafish embryos with reduced HSBP1 levels exhibit elevated levels of Hsf1 activity and expression of heat shock proteins (Hsps). We conclude that HSBP1 plays an essential role during early mouse and zebrafish embryonic development.

Keywords

HSBP1; knockout mice; embryonic stem cells; zebrafish; neural crest

[6]Corresponding Authors: Nahid F. Mivechi, Tel: 706-721-8759; nmivechi@gru.edu; Ali Eroglu, Tel: 706-721-7595; Aeroglu@gru.edu.
[3]Present address: Yale University School of Medicine, Department of Laboratory Medicine BML 458, P.O. Box 208035, 330 Cedar Street, New Haven, CT 06520-8035: jin-na.min@yale.edu.
[4]Present address: Virginia Bioinformatics Institute, Washington St., MC0477, Blacksburg, VA 24061. yanzhang@vt.edu.

Introduction

Heat shock factor binding protein 1 (HSBP1) is a 76 amino acid polypeptide that was originally isolated by a yeast two-hybrid screen to bind to heat shock factor 1 (Hsf1) (Cotto and Morimoto, 1999; Satyal et al., 1998). HSBP1 interacts with the Hsf1 trimerization domain, represses its transcriptional activity, and has a potential role to affect the activities of other proteins containing coiled-coiled motifs (Satyal et al., 1998). NMR analysis of HSBP1 shows that it is a single continuous helix and occurs largely in trimeric form (Tai et al., 2002). Over 60% of HSBP1 protein consists of a highly conserved hydrophobic heptad repeat (Tai et al., 2002) that is represented as a and d in the sequence abcdefg (Tai et al., 2002). The structure of HSBP1 has been resolved at 1.8°A. Amino acid residues 6–53 of HSBP1 form a continuous 11-turn long helix. The helix is self-associated and forms a parallel, symmetrical, triple coiled-coiled helix bundle, assembling further into a dimer of trimers in a head-to-head structure (Liu et al., 2009). HSBP1 is an evolutionarily conserved protein and its function in cells remains unresolved. Recent results indicate that up-regulation of HSBP1 is involved in the gain of a more invasive phenotype following treatment of cells with a mid-region domain of parathyroid hormone-related protein (PTHrP) (Luparello et al., 2003). There are two genes encoding HSBP in *Zea mays*, HSBP2, and EMP2 (Fu et al., 2006). EMP2 mutants are embryonic lethal, presumably due to its requirement to down-regulate heat shock proteins (Hsps) during embryogenesis. HSBP2, however, is induced following exposure to heat shock (Fu et al., 2006).

In this study, we attempted to understand the function of HSBP1 in mouse and zebrafish early embryonic development. Our data indicate that HSBP1 is critical for preimplantation stage of embryonic development. *Hsbp1*$^{-/-}$ ES cells differentiation into embryoid bodies indicate that HSBP1 is involved in the proper organization of the three germ layers during gastrulation. HSBP1 is also involved in correct development of neural crest cells and proper development of the body axis.

Methods and Materials

Construction of targeting vector and generation of mice deficient in the hsbp1 gene

A 15 kilobase pair genomic clone containing more than 3 kilobase pairs of the promoter region and the 4 exons of the murine *hsbp1* gene was isolated from a 129/SvJ mouse genomic library (λ FixII vector, Stratagene, La Jolla, CA) using a mouse *hsbp1* cDNA as probe (Zhang et al., 2002). This genomic clone was used to construct a targeting vector containing a mutant *hsbp1* gene. A 3.3 kilobase pair proximal fragment spanning part of the *hsbp1* promoter and the *hsbp1* start codon was amplified by PCR. A 2.2 kilobase pair fragment of EGFP-neomycin (neo; positive selectable marker) cassette containing *BamH*I and *Cla*I restriction enzyme sites at the 5’- and 3’-termini, respectively, was ligated to the proximal 3 kilobase pair fragment. This construct resulted in an out-of-frame deletion of exons 1 and 2 and intron 1. The expression of EGFP with the poly (A) signal was driven by the *hsbp1* promoter. The neomycin gene was flanked by two *loxP* sites to allow its removal by the cre recombinase and its expression was driven by the thymidine kinase (*tk*) promoter with a simian virus 40 poly (A) signal (Min et al., 2004). The resulting 8.5 kilobase pair fragment (*hsbp1* promoter-*EGFP-neomycin-hsbp1 gene*) was subcloned into the

λDashII-254-2TK vector at the *Xho*I site. The 8.5 kilobase pair fragment in λDashII-254-2TK was flanked by two *tk* genes which were used as a negative selectable marker. The identity of all fragments in the final targeting vector was confirmed by dideoxynucleotide sequencing. The targeting vector was linearized at the unique *Not*I site for embryonic stem (ES) cell transfection. ES cells (D3; Incyte Genomics, St. Louis, MO) were electroporated with the linearized targeting vector and selected for double resistance to G418 (200 μg/ml) and FIAU (ganciclovir, 2 μM) following a standard protocol (Incyte Genomics, St. Louis, MO) (Min et al., 2004). The correct targeting of the resistant ES clones was confirmed by Southern blotting using *EcoRI*-digested genomic DNA and a 500 base pair probe located external to the targeting vector (Figure 1A). Two ES cell clones were microinjected into C57BL/6 blastocysts and several chimeric mice were generated.

All live animal studies were performed in accordance with NIH guidelines for use and care of animals and were approved by the Institutional Animal Care and Use Committee.

Genotype analysis

The genotyping of mice was performed by Southern blotting of tail DNA with an external probe, or by PCR using one common primer (P1; 5'-AGAGATTGAACTCACAGTGTCAG-3'), a primer to detect the wild-type locus (P2; 5'-GCATGGTCTTGGGGTCCGTC-3') and a primer for the EGFP gene (P3; 5'-CGGACTTTGAAGTTCACCTTGAT-3') to identify the mutant gene (see Figure 1A). The expected PCR products for the wild-type and the targeted *hsbp1* loci are fragments of approximately 437 base pairs and 900 base pairs, respectively. For the genotyping of the E0.5 to E3.5 day old embryos, embryos were flushed from the mouse uteri, and each collected in 15 μl of lysis buffer (50 mM KCl, 10 mM Tris-HCl pH8.0, 2mM $MgCl_2$, 0.45 % Nonidet P-40, 0.45% Tween-20 and 100μg/ml Proteinase K). DNA was extracted from cells by incubation at 55°C for 1 hour followed by incubation at 95°C for 10 min. Half of the extracted DNA was then used in the PCR reaction.

Embryo cultures

Timed pregnancies were used to generate pre-implantation embryos. *Hsbp1* heterozygous female mice were superovulated by an intraperitoneal administration of a combination of 5 IU equine chorionic gonadotropin, and 2.5 IU human chorionic gonadotropin followed 48 hours later by an intraperitoneal injection of 7.5 IU human chorionic gonadotropin (PG 600, Intervet, Millsboro, DE or Sigma-Aldrich, St. Louis, MO) alone. Treated females were crossed with heterozygous *hsbp1* males, and the vaginal plug was detected the morning after, which was designated embryonic day 0.5 (E0.5). Two-cell-stage embryos were cultured in bicarbonate-buffered Hypermedium (Eroglu et al., 2009) at 37°C under a humidified gas atmosphere of 5% CO_2 in air for 5 days to evaluate their development to the blastocyst stage.

Preparation of ES cells deficient in hsbp1

To collect a large number of embryos for ES cell derivation, *hsbp1* heterozygous female mice were superovulated as described above and crossed with heterozygous *hsbp1* males. Two-cell-stage embryos were flushed from oviducts and cultured in bicarbonate-buffered

Hypermedium until they reached the blastocyst stage. Briefly, the subsequent steps of ES cell derivation were carried out as follows: blastocysts were cultured in knockout Dulbecco's Modified Eagle Medium (DMEM, Gibco) on irradiated mouse fetal fibroblasts (feeders) plated on gelatin-coated dishes. To promote undifferentiated outgrowth of inner cell mass (ICM) cells, knockout DMEM was supplemented with 1000 IU/mL recombinant murine leukemia inhibitory factor (LIF, Millipore), 25 μM MEK1 inhibitor PD 98059 (LC Laboratories, Woburn, MA), 2 μM GSK-3 inhibitor BIO (Calbiochem, Darmstadt, Germany), 2 mM L-glutamine (Gibco), 0.09 mM β-mercaptoethanol, 1X non-essential amino acids (Gibco), 5% fetal bovine serum (FBS, HyClone, South Logan, UT), 50 IU/mL penicillin, and 50 μg/mL streptomycin. After four days of co-culture, ICM outgrowths were individually collected, dissociated with 0.05% trypsin-EDTA (Gibco), and plated on fresh feeder layers. The resulting undifferentiated colonies were further propagated in the same medium, and then in the absence of MEK1 and GSK-3 inhibitors. The latter medium was termed ES cell medium. Putative ES cell lines were passaged ≥10 times in the ES cell medium, genotyped and characterized by immunofluorescence staining of Oct-4, Nanog, stage specific embryonic antigen 1 (SSEA-1), as well as by alkaline phosphatase (AP) staining (data not shown). Karyotyping was carried out as described in detail elsewhere (Keskintepe et al., 2007). Briefly, ES cell colonies were incubated with 0.1 mg/mL colcemid (Gibco) at 37°C for 1 hour to arrest cells in mitosis at the metaphase stage. ES cells were then dissociated, treated with 0.075 M KCl at 37°C for 20 minutes, and then three times fixed in Carnoy's fixative. The fixed cells were air dried on pre-cleaned slides and stained with Giemsa (Fisher Scientific) for G-banding, and thus for evaluation of their chromosomal normality.

Embryoid bodies (EBs) and teratoma preparation

ES cells were expanded in the aforementioned ES cell medium on a feeder cell layer of irradiated mouse primary fetal fibroblasts that were plated on gelatin-coated 6-well dishes. For EB formation, trypsinized ES and feeder cell mixtures were replated on poly-L-lysine-coated dishes and incubated at 37°C for up to 2 hours, a time period sufficient for the feeder cells to attach to the culture dishes while the ES cells remained unattached. The unattached ES cells were then aspirated, pelleted, and then resuspended in the ES cell culture medium lacking LIF at a density of 20–25 $\times 10^3$ cells/ml. To generate EBs in hanging drops, 35-μl drops from the ES cell suspension were pipetted on an inverted lid of a plastic culture dish (Sharma et al., 2011). Immediately thereafter, the lid was turned over and placed on the bottom part that contained 10 ml PBS to prevent evaporation of the hanging drops. The ES cells in the hanging drops were cultured for 2 to 5 days to form EBs at different sizes, depending on the subsequent experimental needs.

To assess the capacity of *hsbp1*$^{-/-}$ and wild-type ES cells for *in vivo* differentiation and teratoma formation, approximately 2×10^6 cells were subcutaneously injected into the dorsal flanks of athymic nu/nu mice. After three weeks, teratomas were removed, fixed in 4% paraformaldehyde (PFA), and then processed for histology.

ES cell differentiation into neuronal lineage

To differentiate mouse ES cells into the neural lineage, a four-step protocol was employed. First, EB cultures were initiated by culturing dissociated ES cells in hanging drops for 2 days. Thereafter, small EBs were transferred to DMEM/F-12 medium containing 1x N2 /B27 supplements (Invitrogen) and cultured in suspension for 3 days for initial neural induction. Because N2/B27 supplements together contain retinoic acid (RA), insulin, transferrin, and selenite (ITS), additional RA and ITS supplementation was not necessary. The second step involved further neural induction and formation of neural progenitor (NP) rosettes. To achieve this, EBs were plated on type IV collagen and cultured in DMEM/F12 medium containing 1X N2/B27 supplements plus 200 ng/ml noggin for 4 days. At the end of the culture period, EB residues (i.e., non-migrated cells) were mechanically removed and discarded. In the third step, expansion of the NP rosettes and formation of neural tube-like structures were accomplished by trypsinizing and plating migrated cells on polyornithine/ laminin-coated dishes containing DMEM/F12 medium supplemented with 20ng/ml bFGF and 1X N2/B27. In the fourth step, final differentiation was attained by mechanically isolating neural tubes and plating them on polyornithine/laminin-coated dishes containing DMEM/F-12 with 1 mM dbcAMP and 1X N2/B27 for 7 days.

Quantitative real-time PCR

Total RNA was isolated from mouse ES cells, EBs or zebrafish embryos at 12 hpf using TRIZOL reagent (Invitrogen) according to the manufacturer's instructions. cDNAs were generated using iScript cDNA synthesis Kit (BioRad). The primers used are listed in Table S1. A Real-Time PCR System (Applied Biosystems) and SYBR Green PCR supermix were used for the reactions. Samples were normalized to β-actin. Results were presented as mean ± SEM relative to control.

Histology, immunohistochemistry and Western blotting

Embryos recovered at embryonic day (E) 7.5–12.5 or one or two-week-old EBs were embedded in OCT, snap-frozen in a dry ice/2-methylbutane bath, sectioned, air-dried, and fixed in 0.2% glutaraldehyde in PBS (pH 7.3) with 2 mM $MgCl_2$ or 4% PFA for 10 min. For paraffin embedding, EBs were washed with PBS, fixed with 4% PFA at 4°C for 16 hours, rinsed with PBS and placed in Histogel (Richard-Allan Scientific). After processing, EBs were embedded in paraffin. Teratomas were fixed in 4% PFA, processed and embedded in paraffin. Seven-μm tissue sections from each specimen were stained with hematoxylin/eosin (H&E) and subjected to microscopic analyses. For immunohistochemistry, paraffinized tissue sections were deparaffinized in xylene and rehydrated in a series of alcohol-water mixtures. Antigen retrieval was performed by boiling the slides in 10 mM sodium citrate (pH 6.0) including 0.05% Tween-20 for 30 minutes. The tissue sections were then incubated in PBS containing 3% BSA for 1 hour at 25°C. Tissue sections were incubated in primary antibody at 4°C for 16 hours, rinsed with PBS/Tween 20 for 30 minutes and incubated with secondary antibodies conjugated to Alexa Fluor 594 (Molecular Probes) at 25°C for one hour. Tissue sections were mounted with Vectashield mounting medium containing DAPI (Vector Laboratories). Immunostained tissue sections were analyzed by Zeiss Axio Imager (Homma et al., 2007). For teratomas, tissue sections were treated as described above. After

primary antibody treatment, tissue sections were rinsed and incubated with biotinylated secondary antibody for one hour at 25°C. Sections were rinsed and incubated with Extravidin-Alkaline Phosphatase for 30 minutes. Fast red and hematoxylin staining (Sigma) were used to visualize tissue sections (Homma et al., 2007). Primary antibodies used for immunohistochemical staining were as follows: Hsp70 (StressMarq), Hsp90a (Assay Design), Hsf1 (Cell Signaling), Desmin, αSMA (Sigma), NeuN, Nestin, MAP 2A (Millipore), Apolipoprotein E, Keratin 18, Vimentin (Abcam), α-Fetoprotein (R&D Systems), Ki67 (Neomarkers), β-Tubulin III (Epitomics), GFAP (Dako Cytomation), Collagen I and III (Rockland), Troponin, Hsp110, and βActin (Santa Cruz). Western blotting was performed as reported previously (Eroglu et al., 2010). Antibodies used for Western blotting included HSBP1 (Abcam), Hsf1 (Cell Signaling), Hsp110 (Santa Cruz), Hsp90a (Assay Design), and Hsp70 (Stress Marq).

Fish maintenance

Zebrafish, *Danio rerio*, and embryos were maintained under standard conditions as described previously (Detrich et al., 1999). Zebrafish embryos were staged in hours post fertilization (hpf) according to Kimmel, et.al. (Kimmel et al., 1995).

Morpholino and mRNA injections

The zebrafish HSBP1-morpholino (HSBP1 MO) and Hsf1 MO were obtained from Gene Tools LLC (Corvallis, OR). The sequences of the MOs were as follows: HSBP1 MO1 5'-CTGATTTTGGGTCTGTCTGTGCCAT-3'; HSBP1 MO2 5'-TGCACCTGTTTGGGACAAACTGTTA-3'; control MO 5'-CCTCTTACCTCAGTTACAATTTATA-3'; Hsf1 MO 5'CACGGAGAGTTTAGTGATGATTTCT-3'; p53 MO 5'-GCGCCATTGCTTTGCAAGAATTG-3'. The HSBP1 MO1 was designed upstream of ATG (exon 1) in reverse orientation. HSBP1 MO2 spanned 5 bases in exon 2, and 20 bases in intron 1 in the reverse orientation. The MO oligonucleotides were dissolved in 1X Danieau's buffer (Nasevicius and Ekker, 2000) (stock concentration of 20 ng/nl). For MO microinjection, one to two-cell-stage zebrafish embryos were injected with either HSBP1 MO1, HSBP1 MO2, Hsf1 MO, or control MO. The embryos were then fixed at different stages, and gene expression analyses were performed using *in situ* hybridization assay. To determine the required HSBP1 MO1, HSBP1 MO2 or Hsf1 MO concentrations to down-regulate HSBP1 or Hsf1, a series of experiments were performed where embryos were injected with different MO concentrations and survival of the embryos was estimated at 24 hpf (Eroglu et al., 2006). The final concentration of the HSBP1 MO1 used was 2.5 ng, HSBP1 MO2 was 5 ng, and Hsf1 MO was 5 ng (Eroglu et al., 2006), and these were selected since all the MO-injected zebrafish embryos could be rescued following specific mRNA injection (Eroglu et al., 2006). The final concentration of p53 MO that was used was 5ng/embryo (Robu et al., 2007).

For mRNA injections, full-length z*hsbp1* and *zhsf1* mRNAs were synthesized using mMessage mMachine RNA Transcription Kits (Ambion). 500 pg of z*hsbp1* or *zhsf1* mRNA were injected into the egg yolk of the 1–2 cell-stage untreated or MO-treated embryos.

Whole-mount in situ hybridization

Whole-mount *in situ* hybridization was performed as described previously (Oxtoby and Jowett, 1993). Sense and antisense probes (*Hsbp1, Anf2, Engrailed-2, Krox-20, Hlx1, Notail, Foxd3, Snail2* and *Tfap2a* (Eroglu et al., 2006)) were labeled with digoxigenin-UTP (Roche) and visualized with anti-digoxigenin alkaline phosphatase (Boehringer Manheim). To visualize the immunostained embryos, the embryos were cleared in 70% glycerol and photographed using a Leico dissecting microscope.

Statistical analyses

All experiments were performed at least two times. Data are presented as mean ± SEM. Statistical significance between experimental groups was assessed using unpaired two-tailed Student's *t* test, and $p<0.05$ values were considered significant.

Results

Analyses of mice deficient in hsbp1 reveal early embryonic lethality

The targeting vector was designed to remove a portion of the *hsbp1* exon 1 following the ATG codon, exon 2, and intron 1 and insertion of the EGFP reporter gene (Figure 1A). *Hsbp1*$^{+/-}$ mice were generated as described in the Methods and Materials and were intercrossed. Southern blotting or PCR analysis of tail DNA that was extracted from the neonates revealed the absence of any *hsbp1*$^{-/-}$ mice (Figure 1B). Figure 1B shows the lack of HSBP1 expression in ES cells generated from *hsbp1*-deficient embryos (see below) using Western blotting. From a total of 175 live-born progeny that were genotyped, we obtained 46 (26%) *hsbp1*$^{+/+}$, 129 (74%) *hsbp1*$^{+/-}$, and 0 (0%) *hsbp1*$^{-/-}$ mice, indicating that disruption of the *hsbp1* gene results in complete lethality of homozygous mice (Figure S1A). Based on the absence of live born *hsbp1*$^{-/-}$ mice, we anticipated that lesions causing prenatal lethality could be revealed at different stages of embryonic development. To determine the time that lethality occurs in the *hsbp1*-deficient embryos following heterozygote intercrosses, timed pregnancies were terminated at different times post conception. Uteri were analyzed for the presence of resorbed decidua, and embryos were extracted, observed phenotypically, and genotyped. We analyzed 4 litters at E5.0-E5.5, and 17 litters at E7.5-E18.5 (Figure S1). Our results indicated no resorbed embryos at E5.0-E5.5. In addition, we found no *hsbp1*$^{-/-}$ embryos at E5.0 to E5.5, or older (Figure S1A–E). We also analyzed embryos at the blastocyst stage following *hsbp1*$^{+/-}$ intercrosses. Data indicate that from 93 blastocysts that were cultured and genotyped, 57.7% of the *hsbp1*$^{-/-}$ embryos were arrested or degenerated before reaching the blastocyst stage and only 3.8% of the blastocysts hatched (Table S2). These data indicate that the lethality of *hsbp1*$^{-/-}$ embryos occurred at the preimplantation stage.

In order to examine the *hsbp1*-driven *EGFP* expression in the embryos, following heterozygote intercrosses embryos were examined at E0.5 (one-cell stage), E1.5 (2-cell stage), and E3.5 for the presence of *hsbp1-EGFP* expression and genotyped at blastocyst stage. The data presented in Figure 1C–E indicate that *hsbp1- EGFP* is expressed at E0.5, E1.5 in *hsbp1*$^{+/-}$ or *hsbp1*$^{-/-}$*-EGFP* blastocysts. HSBP1 is a maternal factor since no *hsbp1*-

driven *EGFP* expression could be detected until the blastocyst stage in embryos derived from wild-type females crossed with heterozygous males (data not shown).

The expression of *hsbp1*$^{+/-}$-driven *EGFP* continued during later developmental stages at E8.5, E9.5, and E10.5 in the entire embryo (Figure 1F). The *hsbp1* expression was also detected using *in situ* hybridization analyses, confirming the data obtained with the *hsbp1*-EGFP expression pattern (Figure 1G).

Isolation of hsbp1-deficient ES cells

To examine the role of HSBP1 during early embryonic development, 250 E3.5 day-old blastocysts were isolated from *hsbp1*$^{+/-}$ intercrosses. Approximately 50 HSBP1 blastocysts were successfully cultured. Genotyping of ES cell lines indicated 2 *hsbp1*$^{-/-}$ ES lines among the isolated cell lines (Figure S2A). The proliferation of wild-type, *hsbp1*$^{+/-}$, and *hsbp1*$^{-/-}$ ES cells were comparable, and *hsbp1*$^{+/-}$-*EGFP* and *hsbp1*$^{-/-}$-*EGFP* ES cell lines expressed *hsbp1*-driven *EGFP*, confirming that HSBP1 is transcribed in the ES cell lines. These results indicate that HSBP1 is not required for ES cell proliferation. Additionally, cDNA prepared from all the genotypes were tested for the expression of the ES cell markers *Oct4*, *Nanog*, *Sox2*, and β-*catenin*. Data suggest that expression of these essential molecular markers were comparable between all genotypes (Figure S2B). Figure S2C shows the typical karyotype obtained for the isolated ES cell lines.

Hsbp1$^{-/-}$ EBs exhibit defects in lineage-specific development

The differentiation of mouse EBs from ES cells *in vitro* examines the processes of endodermal and ectodermal differentiation. After 2 days in culture, the outer layer appears as primitive endoderm of the blastocysts. At 3–4 days, a layer of basement membrane appears between the endoderm layer and other cells of the EB. Cellular apoptosis starts in the middle of the inner cell mass (ICM) and broadens into the center of the EB (Li et al., 2003). To determine whether development of ES cells into EBs were comparable between *hsbp1*$^{+/+}$ and *hsbp1*$^{-/-}$ cells, ES cells were cultured in differentiating medium for one (early stage EBs) or two (mid-stage EBs) weeks, and the resulting EBs were analyzed following H&E staining (Qin et al., 2009; Sharma et al., 2011). EBs began to form at 3–4 days (equivalent to 5–6-day-old embryos) and the central cavity started to form at 5–7 days (Figure 2A). Morphologically, *hsbp1*$^{+/+}$ and *hsbp1*$^{-/-}$ EBs appeared comparable. The Ki67 immunostaining of one-week-old EBs indicated comparable numbers of proliferating cells between *hsbp1*$^{+/+}$ and *hsbp1*$^{-/-}$ EBs, while *hsbp1*$^{-/-}$ EBs exhibited significantly higher numbers of Ki67-positive cells in the two-week-old EBs (Figure 2B, right panel). In the two-week-old EBs, we found a larger area of Ki67-positive cells in the mesendoderm in *hsbp*$^{-/-}$ compared to *hsbp1*$^{+/+}$ EBs. To examine whether *hsbp1*$^{-/-}$ EBs exhibited a comparable number of cells undergoing apoptosis as *hsbp1*$^{+/+}$ EBs, a TUNEL assay was performed. Our data indicate a significant increase in the number of cells undergoing apoptosis in the two-week-old *hsbp1*$^{-/-}$ EBs compared to *hsbp1*$^{+/+}$ EBs (Figure 2C). Apoptotic cells in *hsbp1*$^{+/+}$ were located in the central area, while *hsbp1*$^{-/-}$ EBs show apoptotic cells in all areas of the EBs.

Hsbp1$^{-/-}$ EBs express reduced endoderm markers

To investigate whether the expression of genes involved in the development of the three germ layers, ectoderm, mesoderm and endoderm, were comparable between *hsbp1*$^{+/+}$ and *hsbp1*$^{-/-}$ EBs, we performed quantitative real-time PCR (qPCR) and immunohistochemical staining analyses for a number of genes known to express in these cell types. In qPCR studies, we found that the mRNA expression of *Keratin-17, Nestin, Emx* and *Otx1*, which are markers of ectoderm, appeared comparable between the genotypes in the one-week-old EBs, while *Pax2* expression *was* significantly ($p<0.05$) higher (Figure S3). In two-week-old *hsbp1*$^{-/-}$ EBs, the expression of *Pax2, Keratin 17, Emx*, and *Otx1* were significantly elevated ($p<0.05$). Among these markers, *Nestin* is specific to neural primordium and begins to express at E7.75 (Zimmerman et al., 1994), while *Otx1* and *Emx* are anterior-posterior forebrain markers and are involved in the induction of dorsal telencephalon (Boyl et al., 2001; Patarnello et al., 1997). *Emx*1/2 transcripts first appear at E8.0–8.5 days, while *Otx1/2* transcripts first appear at E8.0 days.

The mesoderm marker, *Anf*, which expresses in the most anterior part of the embryo during gastrulation and neurulation (Kazanskaya et al., 1997), appeared comparable in the one-week-old EBs, and its transcript levels significantly increased *($p<0.05$)* in the two-week-old *hsbp1*$^{-/-}$ compared to *hsbp1*$^{+/+}$ EBs. In one- or two- week-old EBs, other mesodermal markers such as *Gata-4, Nodal*, and *BMP-4* were comparable between the genotypes. *Pecam* transcripts, which express in the ICM in the blastocysts, was reduced in *hsbp1*$^{-/-}$ *($p<0.01$)* compared to *hsbp1*$^{+/+}$ EBs (Figure S3).

The mRNA expression of endoderm markers such as α-*Fetoprotein* (*AFP*) and *Sox17* were significantly reduced in one-week-old *hsbp1*$^{-/-}$ EBs compared to *hsbp1*$^{+/+}$ EBs (Figure S3). The expression of *AFP, Foxa-2, Apoa-2, and Sox17* were also significantly lower in 2-week-old *hsbp1*$^{-/-}$ EBs compared to *hsbp1*$^{+/+}$ EBs, while the expression of transferrin was lower, but did not reach significance between the genotypes. Both *Sox17* and *Foxa2* are involved in the formation of definitive endoderm, while *A* initially expresses in the primitive endoderm during early post implantation stages, and its expression is maintained in the visceral and parietal endoderm of the yolk sac during gastrulation (Zorn, 2008).

The above data indicate minor changes in the transcripts detected for the ectoderm and mesoderm markers between *hsbp1*$^{-/-}$ and *hsbp1*$^{+/+}$ EBs. However, we found significant reduction in the transcripts of endodermal markers such as *AFP, Foxa2, Apoa2* and *Sox17* in *hsbp1*$^{-/-}$ - compared to *hsbp1*$^{+/+}$ EBs.

To examine further if there was a comparable pattern of expression of ectoderm, mesoderm, and endoderm markers in the two-week-old EBs, we performed immunohistochemical staining of Keratin 18, β$\tilde{}$Tubulin III and Nestin (ectoderm), Desmin (mesoderm), AFP and Apolipoprotein E (ApoE) (endoderm) (Figure 3). Our data indicate that the number of cells positive for neural stem cell marker Nestin was notably increased in two-week-old *hsbp1*$^{-/-}$ EBs compared to *hsbp1*$^{+/+}$, and the cellular organization expressing this marker also appeared altered when the two genotypes were compared. Nestin-positive cells in hsbp1$^{+/+}$ EBs were organized around the central cavity, while Nestin-positive structures extended into the central cavity in *hsbp1*$^{-/-}$ EBs. *In vitro*, Nestin expression is normally found in neural

tube-like structures together with a neuroepithelial cell layer surrounding the cavity (Choi et al., 2005). The expression pattern of other ectodermal markers, such as Keratin-18 and β-Tubulin III, were also altered in *hsbp1*$^{-/-}$ EBs. Keratin 18 expression was confined to the cell layer in the outer endodermal epithelial cells in *hsbp1*$^{+/+}$ EBs, while Keratin 18 expression appeared in multiple layers from the outer layer towards the mesendoderm in *hsbp1*-deficient EBs. β-Tubulin III expression in *hsbp1*$^{+/+}$ EBs was confined to the mesendoderm and absent in the central cavity, but occurred in the mesendoderm-occupying portion of the central area in *hsbp1*$^{-/-}$ EBs.

Expression of the mesodermal marker, Desmin, appeared comparable between *hsbp1*$^{+/+}$ and *hsbp1*$^{-/-}$ EBs (Figure 3). Desmin first appears at E8.25 in the neuroectoderm and is temporarily expressed together with Nestin, Vimentin and Keratin. At E8.5, Desmin is detected in the heart and at E9.0 days, in the somites where it is expressed with Vimentin and Nestin (Kachinsky et al., 1994, 1995).

Embryonic liver originates from the ventral foregut endoderm at E8.0 days of gestation (Zorn, 2008; Zorn and Wells, 2009). A short period of time later, at E8.5-E9.0 days of gestation *in vivo*, the epithelium begins to thicken and expresses Albumin and AFP as the liver diverticulum is formed (Zorn, 2008). *In vitro, AFP* is initially detected in the outer layer of the EBs, but in the older EBs is expressed in small areas inside of the EBs (Choi et al., 2005). The expression of the endodermal markers, AFP and ApoE, were notably reduced in two-week-old *hsbp1*$^{-/-}$ EBs compared to *hsbp1*$^{+/+}$ (Figure 3). In two-week-old EBs, we mainly detected AFP in small groups of cells inside the *hsbp1*$^{+/+}$ EBs, and this was notably reduced in number in *hsbp1*$^{-/-}$ EBs. Apolipoprotein E (ApoE) is a lipid transporter and is liver specific. We observed ApoE expression in the mesendoderm in the *hsbp1*$^{+/+}$ EBs, while its expression could not be detected in *hsbp1*$^{-/-}$ EBs (Figure 3).

The above data indicate that there are differences in the pattern of gene expression and cellular organization in the two-week-old *hsbp1*$^{-/-}$ EBs compared to *hsbp1*$^{+/+}$ EBs. In addition, the expression of some of the ectodermal markers that was tested was enhanced while the expression of the endodermal markers was notably reduced in two-week-old *hsbp1*$^{-/-}$ compared to *hsbp1*$^{+/+}$ EBs.

Role of HSBP1 in ES cell differentiation in vivo

The *in vitro* differentiation analysis of *hsbp1*-deficient ES cells to EBs indicated that the expression of HSBP1 is required for efficient *in vitro* ES cell differentiation into proper organization of ectoderm, mesoderm and endoderm. To test whether differentiation of ES cells into neuronal tissue proceeds normally (or perhaps more efficiently as noted in teratoma formation, see below), we differentiated ES cells into neurons using an *in vitro* culture system. The data provided in Figure 4A–D indicate that *Neu N*-positive cells derived from both *hsbp1*$^{+/+}$ and *hsbp1*$^{-/-}$ ES cells could be generated. However, the generation of *Neu N*, β*Tubulin-III* and *Map-2*-positive cells in *hsbp1*$^{-/-}$ cultures were more robust, perhaps suggesting a better differentiating capability of *hsbp1*$^{-/-}$ ES cells into neuronal-derived tissues compared to wildtype.

To further examine the potential role of HSBP1 during *in vivo* differentiation of ES cells, we used the ES-generated teratomas and examined the cell types derived from *hsbp1*$^{+/+}$ and *hsbp1*$^{-/-}$ germ layers. The data presented in Figure S4A and B indicate that *hsbp1*$^{-/-}$ ES cell-induced teratomas exhibit higher proliferative capacity compared to wild-type ES cells. In addition, the data presented in Figure S4C (a–d) indicate that keratinized tissues were abundant in both genotypes. The abundance of other ectoderm-derived tissues, such as skin and keratinized striated epithelium, were comparable between *hsbp1*$^{+/+}$ and *hsbp1*$^{-/-}$ teratomas (data not shown). The mesoderm-derived tissues, such as adipose tissue, muscle, and cartilage, were also equally abundant in both genotypes (Figure S4C e–h). In the case of endoderm-derived tissues, we observed striated columnar ciliated epithelium and serous gland-like cells in both genotypes (Figure S4C i–l). To identify various cell types and whether they express markers of mesoderm and endoderm, we performed immunohistochemical staining (Figure S5). The data indicate that in *hsbp1*$^{-/-}$ teratomas, more than 50% of the tumor areas contained neuroepithelium-derived cells that were positive for *NeuN* and *GFAP* (Figure S5 c–d and e–f), and the expression of *Keratin-18* (ectoderm marker), *Collagen I* and *III*, and *Troponin-I* and *Desmin* (mesoderm markers) were comparable between the two genotypes (Figure S5g–n). The expression of *AFP* and *ApoE4* (endoderm markers) were notably lower in the *hsbp1*$^{-/-}$ compared to *hsbp1*$^{+/+}$ teratomas (Figure S5o–r).

HSBP1-morpholino-treated zebrafish embryos show critical role for HSBP1 during early development

Comparison between mRNA sequences of HSBP1 in human, mouse, and zebrafish indicate a close homology between these species (Figure S6A). To examine the expression of HSBP1 during development of zebrafish, we performed semi-quantitative RT-PCR and *in situ* hybridization analyses using zebrafish embryos at the indicated times (Figure S6B–C). our results indicate that *HSBP1* is expressed during early zebrafish development, and its expression is more limited to the brain region at 24 hpf.

To examine the role of HSBP1 during zebrafish development, we tested whether HSBP1-morpholino (MO)-treated embryos survive and express early developmental markers (Eroglu et al., 2006). Quantification of the surviving embryos at 24 hpf indicated embryonic lethality in 60% and 67% of the embryos that were injected with HSBP1 MO1 or HSBP1 MO2, respectively. The increased apoptotic cells in the central nervous system were evident using acridine orange staining in HSBP1 MO1- or MO2-treated 24 hpf embryos (Figure S7A and data not shown) (Eroglu et al., 2006). From the surviving embryos, we noted a reduced head size and curved body axis in those embryos that reached 48 hpf (Figure S7A and Table S3). In addition, the *HSBP1* mRNA could rescue HSBP1-MO-treated embryos, suggesting that HSBP1 MO specifically inhibited HSBP1 (Figure S7B). In addition, coinjection of p53 MO (Robu et al., 2007) together with HSBP1-MO1 or MO2 improved the phenotypes of HSBP1 MO-injected embryos by 5–12% (Figure S7A and Table S3). However, coinjection of HSBP1 MO1 or MO2 together with p53-MO did not significantly improve the percentages of embryos surviving at 24 or 48hpf compared to those injected with HSBP1 MO1 or MO2. As the immunoblotting experiment presented in Figure S7C indicates, HSBP1 MO could reduce the expression of zebrafish HSBP1 tested at 24 hpf.

The *in situ* hybridization analyses of control or HSBP1-MO1-injected embryos showed the expression domain of the *Anf* gene (forebrain) (Kazanskaya et al., 1997) to be expanded, while the expression domain of *Eng2* (mid/hind brain) (Erickson et al., 2007) and *Krox20* (rhombomeres 3 and 5) (Sun et al., 2002) appeared notably reduced at 10 hpf (Figure S8). Expression of *Eng2* was absent at 12- and 20- hpf, while *Krox 20* expression was reduced at 12–20 hpf in HSBP1-MO-injected embryos compared to control-MO-injected embryos (Figure S8 a–n). Expression of *Notail* (*Ntl*) (notochord) (T-box transcription factor homologous to mouse Brachyury) (Cabrera et al., 1994) appeared shorter and expanded (Figure S8 o–t). Expression of the *Hlx* gene, which defines large areas encompassing the fore-, mid-, and hind- brain (Hjorth et al., 2002), appeared reduced in HSBP1 MO-injected embryos at 24 hpf compared to control MO. *In situ* hybridization of selected probes was also tested using HSBP1 MO2, and results were comparable (data not shown).

The above data indicate that HSBP1 is critical for survival of the embryos, proper development of the central nervous system and body axis in zebrafish. While regions defining the expression of forebrain-specific markers such as *Anf* appeared increased, expression of other neuronal markers defining the midbrain and hindbrain were reduced.

HSBP1 is required for proper neural crest induction

Neural crest (NC) progenitors are induced at the neural plate border during gastrulation and then separate from other neuronal cell types and begin to express specific genes that define the NC cells (Bronner and LeDouarin, 2012; Sauka-Spengler and Bronner-Fraser, 2008). High levels of Wnt signaling and low levels of BMP are important for the specification of NC cells. Specifically, we analyzed the expression pattern of the NC inducers *Tfap2*α, *Snail2* and *Foxd3* at 12 hpf. *In situ* hybridization analyses of embryos showed that there was a significant increase in the expression domain for these markers in HSBP1 MO1- or MO2-treated embryos compared to control MO-treated embryos (Figure 5A–B). *Tfap2a* is expressed in non-neuronal ectoderm at the ventral side (Wang et al., 2011), and *Foxd3* is expressed in the dorsal side of the ectoderm and mesendoderm as has previously been reported (Wang et al., 2011). The *Snail2* gene belongs to a family of transcriptional repressors and has been shown to respond directly to Wnt signaling and to contain TCF/LEF binding sites. These results indicate that the reduction in HSBP1 leads to enhanced expression of genes that are important in the NC induction downstream of Wnt signaling.

Expression of NC inducers and Hsps in hsbp1$^{-/-}$ mouse EBs and HSBP1-MO-treated zebrafish embryos

As presented in Figure 5, the expression domain of NC inducers was increased in HSBP1-MO-treated zebrafish embryos. To examine whether the expression of NC inducers was also increased in mouse EBs, we examined the expression of *Snail2, Slug, Tfap2a, Foxd3* and *E-cadherin* in one- and two-week-old EBs by qPCR. As the data in Figure 6A indicate, the expression levels of *Snail2* and *Foxd3* genes were significantly increased in *hsbp1*$^{-/-}$ one-week-old EBs compared to wild-type EBs. In two-week-old EBs, the expression levels of *Snail2, Slug, Tfap2a* and *Foxd3* were significantly enhanced. Expression of *E-cadherin*, which is repressed by *Snail2/Slug*, was significantly reduced in two-week-old EBs ($p<0.05$) as expected (Come et al., 2006; Sauka-Spengler and Bronner-Fraser, 2008). The *E-cadherin*

is required for cell-to-cell contact, and reduction in its expression normally increases the epithelial mesenchymal transition (EMT) (Thiery et al., 2009).

We also performed a series of experiments to determine the expression of *Snail2, Slug, Tfap2a, Foxd3, E-cadherin* and *N-cadherin* in zebrafish that had been treated with HSBP1-MO1 using qPCR (Figure 6B). As expected, the expression levels of *Snail2, Slug, Tfap2a*, and *Foxd3* were higher and the level of *E-cadherin* was lower in HSBP1 MO1-treated zebrafish embryos compared to control MO. The level of *N-cadherin*, which is increased in its expression, inhibits the Wnt pathway and cellular proliferation (Hay et al., 2009). As noted before, HSBP1 was isolated to interact with Hsf1 and reduce its transcriptional activity (Satyal et al., 1998). Therefore, to probe the possibility that HSBP1 effects could be in part due to Hsf1 up-regulation, we also tested if Hsf1 MO-treated zebrafish embryos would show reduced NC markers relative to control MO. The data in Figure 6B indicate that this is what we observed.

Increased Hsf1 activity (as evidenced by an increase in the expression of its downstream target genes, Hsps) (Zhang et al., 2002) was also investigated in ES cells and in one- and two-week-old EBs (Figure 6C) and in 12 hpf zebrafish embryos (Figure 6E). The data indicate that, indeed, the level of specific Hsps was significantly higher in the two-week-old EBs (Figure 6C), and in HSBP1-MO-treated embryos compared to control MO (Figure 6E). Hsf1 MO effectively reduced the expression level of Hsps (Figure 6E). Western blot analyses of Hsf1, Hsp110, Hsp90α, and Hsp70i also showed increased hyper-phosphorylated form of Hsf1, which is evidence of its increased activity, and a 3-, 6-, and 5-fold increase in the levels of Hsp110, Hsp90α and Hsp70i, in *hsbp1*$^{-/-}$ ES cells relative to wild-type, respectively (Figure 6D).

The above data indicate that changes in HSBP1 levels affect the expression of both mouse and zebrafish NC inducers. Furthermore, when the HSBP1 level is reduced, Hsf1 activity is induced, as evidenced by an increase in the expression level of Hsps.

Discussion

HSBP1 is a 76 amino acid polypeptide containing heptad repeats that has been shown to interact and repress Hsf1 activity (Satyal et al., 1998; Tai et al., 2002). However, HSBP1 can potentially also interact with other transcriptional activators, repressors, and cytoskeletal proteins and modulates their activities. Thus far, however, the function of HSBP1 *in vivo* has remained elusive. In this study, we examined the role of HSBP1 during early embryonic development in mouse and zebrafish, where the level of HSBP1 was either completely reduced using gene knockout technology or partially reduced using morpholino oligonucleotides. Our results indicate that in the mouse, HSBP1 is critical for preimplantation stage of embryonic development. HSBP1 is expressed in ES cells and throughout early embryonic development in the entire embryo. In addition, although we detected the ES cells' differentiation into EBs to occur, we found defects in the organization of the germ layers and reduction in the expression of definitive endodermal markers. The one and/or two-week-old *Hsbp1*-deficient EBs exhibited significant reduction in the endodermal markers *Sox17, Foxa2*, and *Apoa2* (Zorn, 2008). During development of

endoderm, Nodal signaling induces a number of transcription factors, including *Sox17, Foxa2, eomesodermin*, and *GATA-6* (Zorn, 2008). Expression of these factors affects segregation of endoderm and mesoderm and commits cells to the endoderm lineage. *Foxa2* expression is needed for the development of anterior endoderm as its deletion leads to embryos lacking foregut endoderm. *Foxa2* is also known to bind *Albumin* gene enhancer elements, facilitating its transcription (Bossard and Zaret, 1998; Zorn, 2008). *Sox17* expression is needed for the development of posterior endoderm (Zorn, 2008). *Apolipoprotein A2 (Apoa2)* belongs to the high-density lipoprotein family, is liver-specific, and is significantly reduced in *hsbp1*-deficient EBs. We have also found an observable reduction in expression of the liver-specific markers, *AFP* and *ApoE*, in the one and/or two-week-old EBs and teratomas. In general, our data is consistent with a role for murine HSBP1 during development of endoderm.

In terms of the role of HSBP1 during zebrafish development, we have found that HSBP1 is expressed uniformly in the embryo until 16–24 hpf, where HSBP1 expression gradually becomes limited to the anterior region of the embryo. Our data further show that HSBP1 knockdown leads to an increase in the expression domain of the forebrain-specific transcription factor *Anf*, and loss or severe reduction in the expression of *engrailed 2* (mid/hind brain-specific marker) and *krox 20* (hind-brain marker) (Oxtoby and Jowett, 1993), and the homoebox transcription factor *Hlx* (Fjose et al., 1994). The expression domain of the notochord-specific marker *Notail* (*ntl*) (Schulte-Merker et al., 1992) shows reduced length and expansion at 10 hpf, resulting in the embryos showing a curved body axis observed at 24–48 hpf. This may suggest a role for HSBP1 in convergent extension (CE) movement during gastrulation. During gastrulation, cells that eventually give rise to the ectoderm, mesoderm and endoderm go through an organized migration towards the dorsal side (convergence), and those cells intercalate around the dorsal midline, causing elongation of the embryo along its antero-posterior body axis (extension). Defects in CE movements leads to shortening of the body axis and widening of the mediolateral side (Tada and Heisenberg, 2012). Using the expression of *ntl* as marker, previous studies have shown that when CE movement is inhibited, the notochord domain becomes shortened along the anterior-posterior axis and widened along the mediolateral side (Heisenberg et al., 2000). The non-canonical Wnt signaling plays a critical function in CE movements (Tada and Heisenberg, 2012).

Knockdown of zebrafish HSBP1 leads to the expansion of the domain of cells expressing the NC inducers, *tfap2a, snail2* and *foxd3*. NC cells are an embryonic cell population that arises at the end of gastrulation at the border of the neural plate and non-neural ectoderm. They migrate and differentiate into various cell types, such as neurons, glia, melanocytes, bone and cartilage (Sauka-Spengler and Bronner-Fraser, 2008). NC cells undergo induction, specification, and terminal differentiation (Meulemans and Bronner-Fraser, 2004), and their induction occurs during early development through the activity of signaling pathways such as Wnt, FGF, Notch and BMP (Wang et al., 2011). Inhibition of the Wnt/β-catenin pathway inhibits NC formation both in mouse and zebrafish (Wang et al., 2011). Ectopic expression of Wnt family members leads to an increase in NC progenitors. These and other data suggest that Wnt signaling is sufficient for the induction of NC cells (Garcia-Castro et al., 2002).

During development, activation of Wnt signaling leads to the BRG1 chromatin remodeling complex interacting with nuclear β-catenin and the promoter of TCF/LEF transcription factors, leading to an increase in the expression of downstream target genes such as *Snail2*, *Tfap2*α, and *Foxd3* (Sauka-Spengler and Bronner-Fraser, 2008). Activation of Wnt/BRG1/β-catenin/TCF/LEF and expression of their downstream target genes, such as *Snail/Slug*, has been shown to induce EMT (Eroglu et al., 2006; Sauka-Spengler and Bronner-Fraser, 2008; Thiery and Sleeman, 2006). EMT is a process where epithelial cells convert to mesenchymal cells during development and cancer progression (Huang et al., 2012). Once the neural tube closes, cells undergo EMT within the neural epithelium and migrate to form multiple cellular lineages (Bronner and LeDouarin, 2012; Sauka-Spengler and Bronner-Fraser, 2008). The genes involved in NC induction and EMT function in altering cell-to-cell junctions. One such example occurs when the *Snail* transcriptional repressor inhibits *E-cadherin* expression, which results in the inhibition of EMT (Sauka-Spengler and Bronner-Fraser, 2008). As noted before, HSBP1 has been shown to suppress Hsf1 transcriptional activity through their direct protein-protein interactions. Our data show an increase in Hsf1 activity upon *hsbp1* gene knockout in ES cells. Through qPCR of cDNA prepared from *hsbp1*-deficient EBs and zebrafish embryos carrying knockdown of HSBP1, we were able to show that reduced levels of HSBP1 correlated with an increase in the expression of NC inducers as well as an increase in the level of specific Hsps in both models. Normally, an increase in the expression of *Snail2* results in the reduction of its downstream target, *E-cadherin*. However, the reduction in *E-cadherin* that we observed in Figure S3 appears to be only 20–30% relative to wild type and less than expected. Additional studies are needed to examine the function of HSBP1 during EMT. The role of Hsf1 and its downstream targets, Hsps, during early central nervous system development, NC induction, or EMT has not been extensively investigated. However, we have recently found that ablation of Hsf1 leads to a reduction in EMT and metastasis in ERBB2-expressing mammary tumors as evidenced by the reduction in *Snail/Slug* expression and an increase in the expression of *E-cadherin*, suggesting that Hsf1 activity and Hsp expression is required for EMT (Xi et al., 2012).

In conclusion, we provide evidence that HSBP1 is critical for early embryonic development and potentially affects the Wnt signaling pathway, leading to the expansion of the NC inducers that express in specific developmental stages in both mouse embryos during and after gastrulation, as well as in zebrafish embryos at and beyond 12 hpf. HSBP1 reduction leads to defects in neurodevelopment in zebrafish as evidenced by the expression pattern of specific forebrain, mid- and hind-brain markers. HSBP1 reduction in both mouse and zebrafish also leads to increased Hsf1 activity and, therefore, the phenotype of *hsbp1*-deficient mice or zebrafish could at least be due in part to elevated activity of Hsf1.

Supplementary Material

Refer to Web version on PubMed Central for supplementary material.

Acknowledgments

This work was supported by VA Award 1I01BX000161, and in part by NIH grants CA062130, CA132640 (N.F.M.) and CA121951 (D.M.). The authors wish to thank Dr. Ellen K. LeMosy at GRU for providing materials.

References

Bossard P, Zaret KS. GATA transcription factors as potentiators of gut endoderm differentiation. Development. 1998; 125:4909–4917. [PubMed: 9811575]

Boyl PP, Signore M, Annino A, Barbera JP, Acampora D, Simeone A. Otx genes in the development and evolution of the vertebrate brain. Int J Dev Neurosci. 2001; 19:353–363. [PubMed: 11378295]

Bronner ME, LeDouarin NM. Development and evolution of the neural crest: an overview. Developmental biology. 2012; 366:2–9. [PubMed: 22230617]

Cabrera CV, Alonso MC, Huikeshoven H. Regulation of scute function by extramacrochaete in vitro and in vivo. Development. 1994; 120:3595–3603. [PubMed: 7821225]

Choi D, Lee HJ, Jee S, Jin S, Koo SK, Paik SS, Jung SC, Hwang SY, Lee KS, Oh B. In vitro differentiation of mouse embryonic stem cells: enrichment of endodermal cells in the embryoid body. Stem cells. 2005; 23:817–827. [PubMed: 15917477]

Come C, Magnino F, Bibeau F, De Santa Barbara P, Becker KF, Theillet C, Savagner P. Snail and slug play distinct roles during breast carcinoma progression. Clin Cancer Res. 2006; 12:5395–5402. [PubMed: 17000672]

Cotto JJ, Morimoto RI. Stress-induced activation of the heat-shock response: cell and molecular biology of heat-shock factors. Biochem Soc Symp. 1999; 64:105–118. [PubMed: 10207624]

Detrich HW 3rd, Westerfield M, Zon LI. Overview of the Zebrafish system. Methods Cell Biol. 1999; 59:3–10. [PubMed: 9891351]

Erickson T, Scholpp S, Brand M, Moens CB, Waskiewicz AJ. Pbx proteins cooperate with Engrailed to pattern the midbrain-hindbrain and diencephalic-mesencephalic boundaries. Developmental Biology. 2007; 301:504–517. [PubMed: 16959235]

Eroglu A, Bailey SE, Toner M, Toth TL. Successful cryopreservation of mouse oocytes by using low concentrations of trehalose and dimethylsulfoxide. Biol Reprod. 2009; 80:70–78. [PubMed: 18815355]

Eroglu B, Moskophidis D, Mivechi NF. Loss of Hsp110 leads to age-dependent tau hyperphosphorylation and early accumulation of insoluble amyloid beta. Molecular and Cellular Biology. 2010; 30:4626–4643. [PubMed: 20679486]

Eroglu B, Wang G, Tu N, Sun X, Mivechi NF. Critical role of Brg1 member of the SWI/SNF chromatin remodeling complex during neurogenesis and neural crest induction in zebrafish. Dev Dyn. 2006; 235:2722–2735. [PubMed: 16894598]

Fjose A, Izpisua-Belmonte JC, Fromental-Ramain C, Duboule D. Expression of the zebrafish gene hlx-1 in the prechordal plate and during CNS development. Development. 1994; 120:71–81. [PubMed: 7907015]

Fu S, Rogowsky P, Nover L, Scanlon MJ. The maize heat shock factor-binding protein paralogs EMP2 and HSBP2 interact non-redundantly with specific heat shock factors. Planta. 2006; 224:42–52. [PubMed: 16331466]

Garcia-Castro MI, Marcelle C, Bronner-Fraser M. Ectodermal Wnt function as a neural crest inducer. Science. 2002; 297:848–851. [PubMed: 12161657]

Hay E, Laplantine E, Geoffroy V, Frain M, Kohler T, Muller R, Marie PJ. N-cadherin interacts with axin and LRP5 to negatively regulate Wnt/beta-catenin signaling, osteoblast function, and bone formation. Molecular and Cellular Biology. 2009; 29:953–964. [PubMed: 19075000]

Heisenberg CP, Tada M, Rauch GJ, Saude L, Concha ML, Geisler R, Stemple DL, Smith JC, Wilson SW. Silberblick/Wnt11 mediates convergent extension movements during zebrafish gastrulation. Nature. 2000; 405:76–81. [PubMed: 10811221]

Hjorth JT, Connor RM, Key B. Role of hlx1 in zebrafish brain morphogenesis. Int J Dev Biol. 2002; 46:583–596. [PubMed: 12141447]

Homma S, Jin X, Wang G, Tu N, Min J, Yanasak N, Mivechi NF. Demyelination, astrogliosis, and accumulation of ubiquitinated proteins, hallmarks of CNS disease in hsf1-deficient mice. J Neurosci. 2007; 27:7974–7986. [PubMed: 17652588]

Huang RY, Chung VY, Thiery JP. Targeting pathways contributing to epithelial-mesenchymal transition (EMT) in epithelial ovarian cancer. Curr Drug Targets. 2012; 13:1649–1653. [PubMed: 23061545]

Kachinsky AM, Dominov JA, Miller JB. Myogenesis and the intermediate filament protein, nestin. Developmental biology. 1994; 165:216–228. [PubMed: 8088440]

Kachinsky AM, Dominov JA, Miller JB. Intermediate filaments in cardiac myogenesis: nestin in the developing mouse heart. The journal of histochemistry and cytochemistry : official journal of the Histochemistry Society. 1995; 43:843–847. [PubMed: 7542682]

Kazanskaya OV, Severtzova EA, Barth KA, Ermakova GV, Lukyanov SA, Benyumov AO, Pannese M, Boncinelli E, Wilson SW, Zaraisky AG. Anf: a novel class of vertebrate homeobox genes expressed at the anterior end of the main embryonic axis. Gene. 1997; 200:25–34. [PubMed: 9373136]

Keskintepe L, Norris K, Pacholczyk G, Dederscheck SM, Eroglu A. Derivation and comparison of C57BL/6 embryonic stem cells to a widely used 129 embryonic stem cell line. Transgenic Res. 2007; 16:751–758. [PubMed: 17701442]

Kimmel CB, Ballard WW, Kimmel SR, Ullmann B, Schilling TF. Stages of embryonic development of the zebrafish. Dev Dyn. 1995; 203:253–310. [PubMed: 8589427]

Li S, Edgar D, Fassler R, Wadsworth W, Yurchenco PD. The role of laminin in embryonic cell polarization and tissue organization. Developmental Cell. 2003; 4:613–624. [PubMed: 12737798]

Liu X, Xu L, Liu Y, Tong X, Zhu G, Zhang XC, Li X, Rao Z. Crystal structure of the hexamer of human heat shock factor binding protein 1. Proteins. 2009; 75:1–11. [PubMed: 18767159]

Luparello C, Sirchia R, Pupello D. PTHrP [67–86] regulates the expression of stress proteins in breast cancer cells inducing modifications in urokinase-plasminogen activator and MMP-1 expression. J Cell Sci. 2003; 116:2421–2430. [PubMed: 12724357]

Meulemans D, Bronner-Fraser M. Gene-regulatory interactions in neural crest evolution and development. Developmental Cell. 2004; 7:291–299. [PubMed: 15363405]

Min JN, Zhang Y, Moskophidis D, Mivechi NF. Unique contribution of heat shock transcription factor 4 in ocular lens development and fiber cell differentiation. Genesis. 2004; 40:205–217. [PubMed: 15593327]

Nasevicius A, Ekker SC. Effective targeted gene 'knockdown' in zebrafish. Nat Genet. 2000; 26:216–220. [PubMed: 11017081]

Oxtoby E, Jowett T. Cloning of the zebrafish krox-20 gene (krx-20) and its expression during hindbrain development. Nucleic Acid Research. 1993; 21:1087–1095.

Patarnello T, Bargelloni L, Boncinelli E, Spada F, Pannese M, Broccoli V. Evolution of Emx genes and brain development in vertebrates. Proc Biol Sci. 1997; 264:1763–1766. [PubMed: 9447733]

Qin J, Guo X, Cui GH, Zhou YC, Zhou DR, Tang AF, Yu ZD, Gui YT, Cai ZM. Cluster characterization of mouse embryonic stem cell-derived pluripotent embryoid bodies in four distinct developmental stages. Biologicals. 2009; 37:235–244. [PubMed: 19339198]

Robu ME, Larson JD, Nasevicius A, Beiraghi S, Brenner C, Farber SA, Ekker SC. p53 activation by knockdown technologies. PLoS genetics. 2007; 3:e78. [PubMed: 17530925]

Satyal SH, Chen D, Fox SG, Kramer JM, Morimoto RI. Negative regulation of the heat shock transcriptional response by HSBP1. Genes Dev. 1998; 12:1962–1974. [PubMed: 9649501]

Sauka-Spengler T, Bronner-Fraser M. A gene regulatory network orchestrates neural crest formation. Nat Rev Mol Cell Biol. 2008; 9:557–568. [PubMed: 18523435]

Schulte-Merker S, Ho RK, Herrmann BG, Nusslein-Volhard C. The protein product of the zebrafish homologue of the mouse T gene is expressed in nuclei of the germ ring and the notochord of the early embryo. Development. 1992; 116:1021–1032. [PubMed: 1295726]

Sharma S, Szurek EA, Rzucidlo JS, Liour SS, Eroglu A. Cryobanking of embryoid bodies to facilitate basic research and cell-based therapies. Rejuvenation Res. 2011; 14:641–649. [PubMed: 21978080]

Sun Z, Shi K, Su Y, Meng A. A novel zinc finger transcription factor resembles krox-20 in structure and in expression pattern in zebrafish. Mech Dev. 2002; 114:133–135. [PubMed: 12175499]

Tada M, Heisenberg CP. Convergent extension: using collective cell migration and cell intercalation to shape embryos. Development. 2012; 139:3897–3904. [PubMed: 23048180]

Tai LJ, McFall SM, Huang K, Demeler B, Fox SG, Brubaker K, Radhakrishnan I, Morimoto RI. Structure-function analysis of the heat shock factor-binding protein reveals a protein composed

solely of a highly conserved and dynamic coiled-coil trimerization domain. J Biol Chem. 2002; 277:735–745. [PubMed: 11679589]

Thiery JP, Acloque H, Huang RY, Nieto MA. Epithelial-mesenchymal transitions in development and disease. Cell. 2009; 139:871–890. [PubMed: 19945376]

Thiery JP, Sleeman JP. Complex networks orchestrate epithelial-mesenchymal transitions. Nat Rev Mol Cell Biol. 2006; 7:131–142. [PubMed: 16493418]

Wang WD, Melville DB, Montero-Balaguer M, Hatzopoulos AK, Knapik EW. Tfap2a and Foxd3 regulate early steps in the development of the neural crest progenitor population. Developmental Biology. 2011; 360:173–185. [PubMed: 21963426]

Xi C, Hu Y, Buckhaults P, Moskophidis D, Mivechi NF. Heat Shock Factor Hsf1 cooperates with ErbB2 (Her2/Neu) protein to promote mammary tumorigenesis and metastasis. J Biol Chem. 2012; 287:35646–35657. [PubMed: 22847003]

Zhang Y, Huang L, Zhang J, Moskophidis D, Mivechi NF. Targeted disruption of hsf1 leads to lack of thermotolerance and defines tissue-specific regulation for stress-inducible Hsp molecular chaperones. J Cell Biochem. 2002; 86:376–393. [PubMed: 12112007]

Zimmerman L, Parr B, Lendahl U, Cunningham M, McKay R, Gavin B, Mann J, Vassileva G, McMahon A. Independent regulatory elements in the nestin gene direct transgene expression to neural stem cells or muscle precursors. Neuron. 1994; 12:11–24. [PubMed: 8292356]

Zorn, AM. Liver development. Cambridge (MA): StemBook; 2008.

Zorn AM, Wells JM. Vertebrate endoderm development and organ formation. Annual Review of Cell and Developmental Biology. 2009; 25:221–251.

Highlights

- We have disrupted heat shock factor binding protein 1 (HSBP1) in mice
- Data show that HSBP1 is critical for survival of the organism
- Data show that HSBP1 is critical for developing endoderm
- Data show that HSBP1 is critical for developing neural crest cells
- Effects of HSBP1 disruption on embryo may in part be due to elevated Hsf1 activity

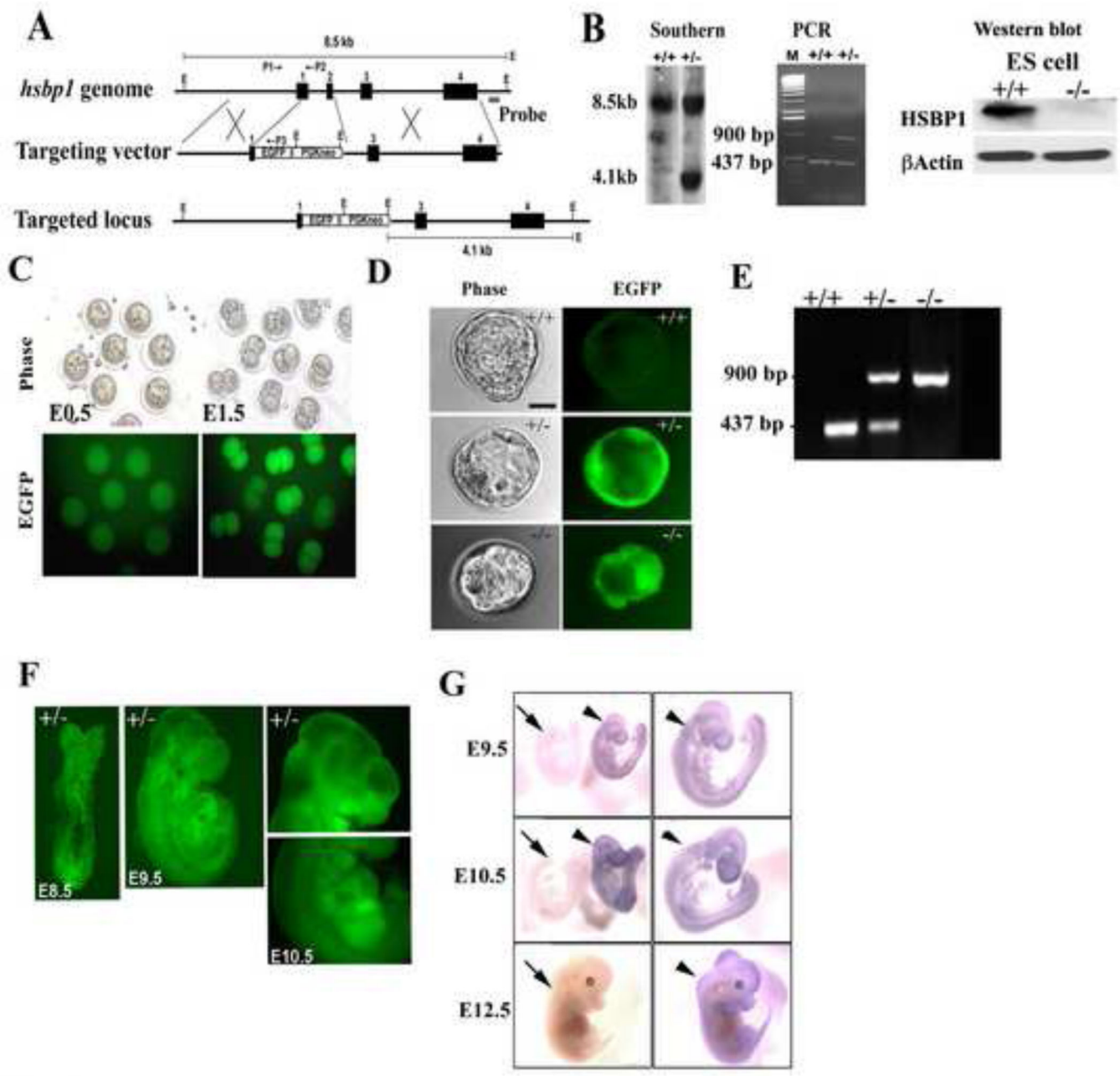

Figure 1. *Hsbp1*-deficient mice exhibit early embryonic lethality

(A) Schematic diagram of wild-type *hsbp1* locus, targeting vector, and the predicted targeted allele following homologous recombination. Exons are indicated by black boxes (1–4). Location of the probe used for Southern blotting and the PCR primers P1, P2, and P3 used for genotyping the mutant mice are indicated. Locations of the EGFP and neomycin genes are indicated.

(B) Southern blotting: *EcoRI*-digested tail DNA from wild-type (+/+) or *hsbp1* heterozygote (+/−) was hybridized with an external probe to yield the predicted fragments, 8.5 kb for +/+, and 4.1 kb for mutant $hsbp1^{+/-}$; PCR: genotyping of tail DNA prepared from +/+, or $hsbp1^{+/-}$ amplifies fragments of 900 bp for the targeted *hsbp1* allele, and 437 bp for the

wild-type allele. Western blotting: extracts were prepared from +/+ and −/− ES cells and show reduction in HSBP1 expression in *hsbp1*-deficient cells. βActin is loading control.
(C) Phase contrast (upper panels) and EGFP expression (lower panels) of $hsbp1^{+/-}$ embryos from $hsbp1^{+/-}$ intercrosses at E0.5 and E1.5 days.
(D) Phase contrast (left panels) and EGFP expression (right panels) in $hsbp1^{+/+}$, $hsbp1^{+/-}$ and $hsbp1^{-/-}$ blastocysts.
(E) Genotyping of DNA extracts of individual blastocysts showing the presence of $hsbp1^{+/+}$, $hsbp1^{+/-}$ and $hsbp1^{-/-}$ blastocysts.
(F–G) Embryos were extracted from $hsbp1^{+/-}$ intercrosses following timed pregnancies. Panel F shows EGFP expression in the E8.5, E9.5 and E10.5 embryos. Panel G shows *in situ* hybrdization of embryos at the indicated stages using sense (arrows) or antisense (arrowheads) HSBP1 as probes.

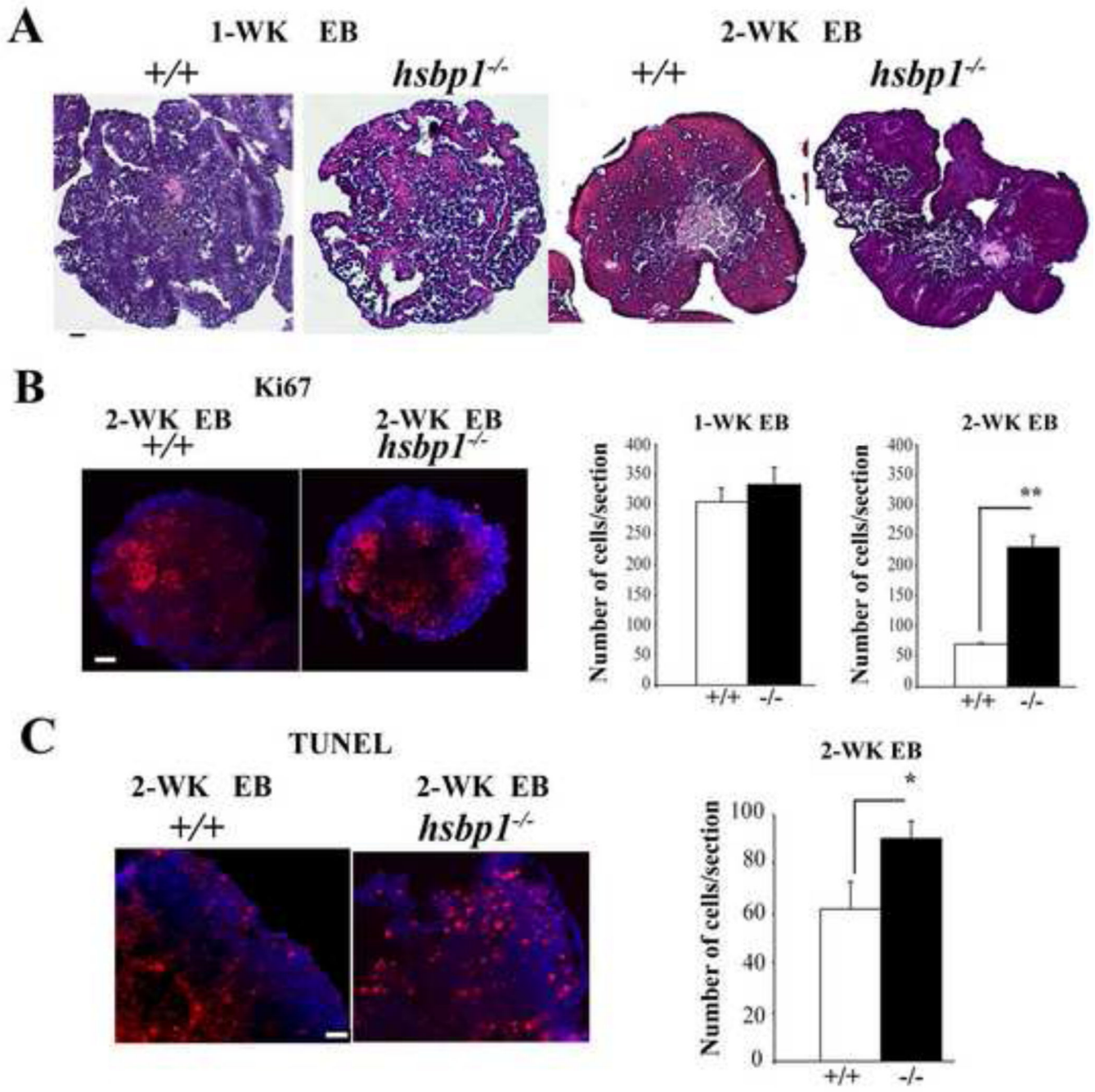

Figure 2. *Hsbp1*-deficient embryoid bodies exhibit increased cellular apoptosis

(A) H& E staining of tissue sections of one- and two-week-old *hsbp1*$^{+/+}$ and *hsbp1*$^{-/-}$ embryoid bodies (EBs). Scale bars: 50 μm.

(B) Tissue sections of two-week-old (2-WK) EBs immunostained using antibody to Ki67. Right panels show quantification of cells positive for Ki67 in one- and two-week old (1-WK and 2-WK) EBs for the indicated genotypes. Scale bars: 50 μm.

(C) Tissue sections of two-week-old EBs immunostained using TUNEL. Bar= 25μm. Right panel shows quantification of positively stained cells per section.

In all panels, bars are mean +/− SEM. Statistical analyses were performed using Student *t*-tests. *$p<0.05$; **$p<0.01$.

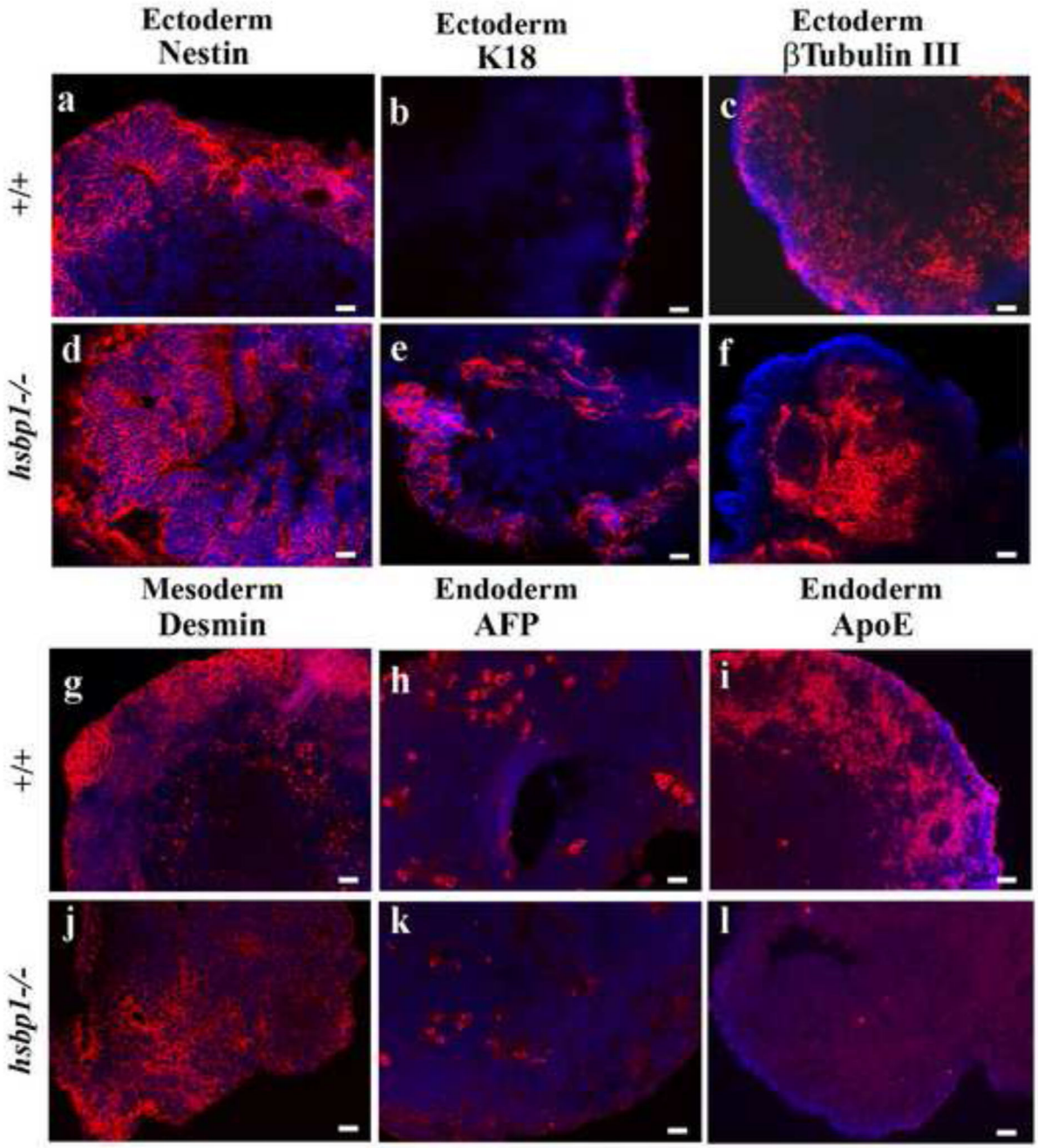

Figure 3. Two-week-old embryoid bodies (EBs) exhibit defects in the expression of endoderm markers

Tissue sections of 2-week-old EBs were immunostained using primary antibody to the indicated markers. Expression of the ectoderm markers, Nestin (a, d), Keratin 18 (K18) (b, e) and β-Tubulin III (e, f); mesoderm marker, Desmin (g, j) and endoderm markers, α-Fetoprotein (AFP) (h, k) and ApoE (i, l) are indicated. Scale bars: 20 μm

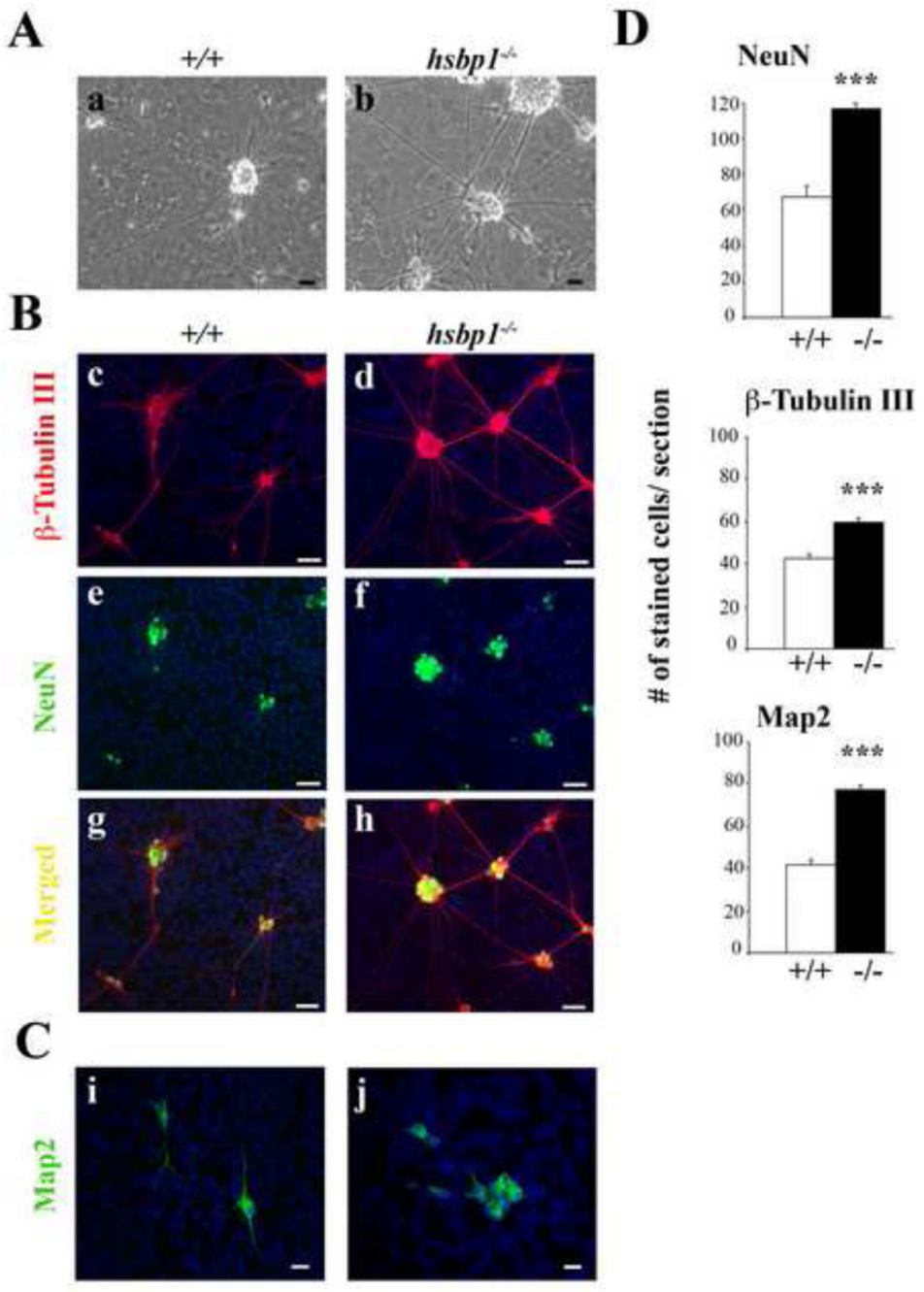

Figure 4. *Hsbp1*$^{-/-}$ ES cell differentiation into neural tissue *in vitro*

(A) Phase-contrast photographs of differentiated *hsbp1*$^{+/+}$ and *hsbp*1$^{-/-}$ ES cells (a–b). Scale bar: 50 μm.

(B) Immunofluorescence staining for β-Tubulin III (Red; c–d) and Neu N (Green; e–f), and nuclear staining (DAPI, blue) of differentiated *hsbp1*$^{+/+}$ and *hsbp*1$^{-/-}$ ES cells. Merged immunofluorescence of β-Tubulin III and NeuN are presented in g–h. Scale bars: 50 μm.

(C) Immunofluorescence staining of Map2 in differentiated *hsbp1*$^{+/+}$ (i) and *hsbp*1$^{-/-}$ (j) ES cells. Scale bars: 20 μm

(D) Quantification of NeuN, β-Tubulin III and Map2 in differentiated *hsbp1*$^{+/+}$ and *hsbp*1$^{-/-}$ ES cells. Bars are mean +/− SEM. Statistical analyses were performed using Student *t*-tests. ****p<0.0001*.

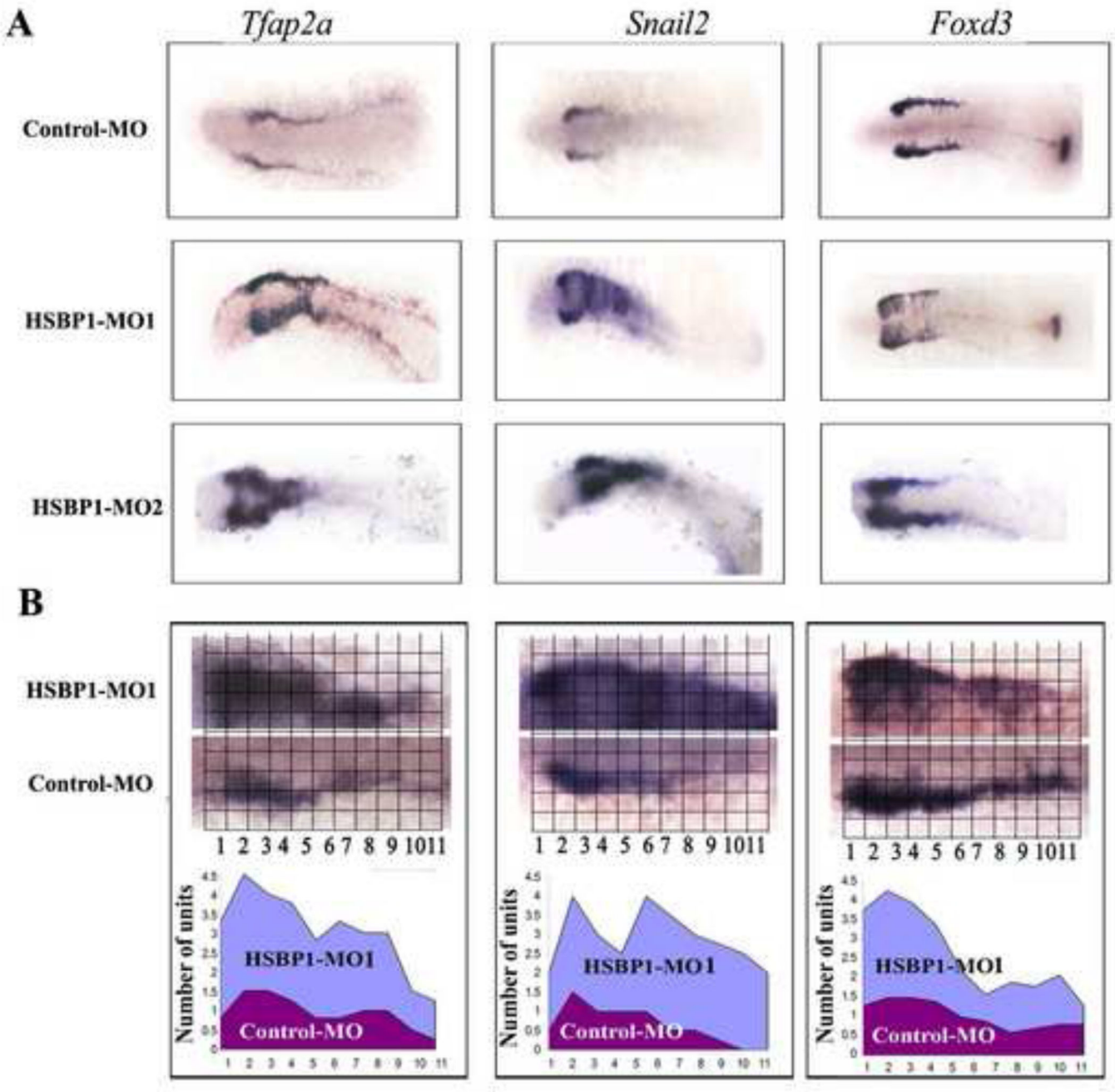

Figure 5. HSBP1-MO-treated zebrafish embryos exhibit increased cellular domains expressing markers representing NC inducers

In situ hybridization analyses showing the expression of the indicated genes in the embryos at 12 hpf stage.

(A) Expression of NC inducers in control MO- and HSBP1 MO1 and MO2- injected embryos. In all panels, dorsal views of the embryos show expression of *Tfap2a*, *Snail2* or *Foxd3*. A total of 2000 embryos were injected and 100 embryos were used per probe for the *in situ* hybridization analyses. No nonspecific hybridization was observed with sense probes (data not shown). Morphant phenotypes were more than 90%, n=40. Mag. 40×.

(B) Quantification of the expression of NC inducers in control MO- and HSBP1 MO1-injected embryos. For data quantification, photos were subdivided and the number of squares was quantified in both Y and X-axis. In the lower panels, numbers in the X-axis correspond to the numbers in the upper panels.

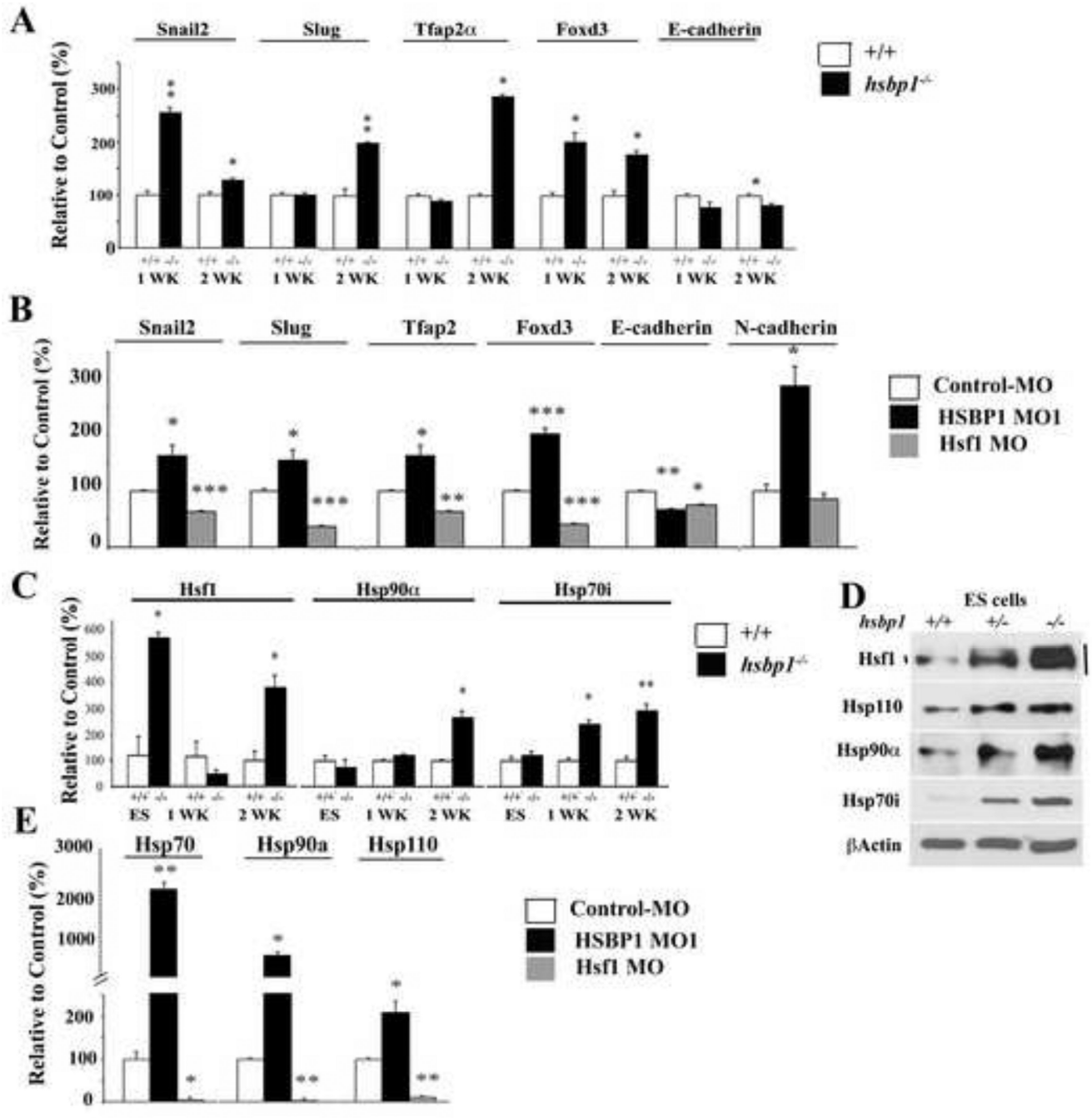

Figure 6. Gene expression profile of NC-inducers and Hsps in mouse EBs and zebrafish embryos

(A) Total RNA was isolated from one- and two-week-old EBs, and cDNAs were subjected to qPCR for the indicated genes.

(B) Total RNA was isolated from the control MO, HSBP1 MO or Hsf1 MO -treated embryos at 12 hpf, and the cDNAs were subjected to qPCR for the indicated genes.

(C) Total RNA was isolated from ES cells or one- or two-week old EBs and the cDNAs were subjected to qPCR for the indicated genes.

(D) ES cell lysates from *hsbp1*$^{+/+}$, $^{+/-}$ and $^{-/-}$ were subjected to immunoblotting to examine the levels of the indicated proteins. Hsf1-retarded mobility shifts indicate its increased activity.

(E) Total RNA was isolated from the control MO, HSBP1 MO or Hsf1 MO -treated embryos at 12 hpf, and the cDNAs were subjected to qPCR for the indicated genes.

In all panels, bars are mean +/− SEM. Statistical analyses were performed using Student *t*-tests. **p<0.05*; ***p<0.01* and ****p<0.001*.